Design and analysis of Wedge-enhanced Raman spectroscopy substrate*

MA A-ning (马阿宁)[1]**, **WEI Wen-jing** (魏文静)[1,2], **PENG Si-chang** (彭嗣昌)[1], **LI Yue-e** (李月娥)[1], **CAI Ke-su** (蔡可苏)[1], **WANG Zhong** (王忠)[1], **and MU Xi-jiao** (穆希皎)[1]

1. School of Information Science and Engineering, Lanzhou University, Lanzhou 730000, China

2. China Mobile Communication Corporation, Lanzhou 730000, China

(Received 29 May 2020; Revised 29 July 2020)

Here, a novel Au Wedge-enhanced Raman spectroscopy (WERS) substrate is proposed. The electric field enhancement factor and the effective mode field radius with varying geometry parameters are investigated. The proper excitation wavelength 633 nm is obtained. The practical application of WERS substrate is discussed. The Au WERS not only can provide a continuous extremely highly localized electric field as surface-enhanced Raman scattering (SERS) hotspots, but also can offer 10 orders of magnitude of SERS enhancement factor. The corresponding results reveal that WERS substrate will be widely applied in optics, biology, chemistry and other fields.

Document code: A **Article ID:** 1673-1905(2021)05-0262-4

DOI https://doi.org/10.1007/s11801-021-0087-5

Surface-enhanced Raman scattering (SERS) is a technique that enhances Raman signal as much as 10^{10}—10^{11} by adsorbing analytes of interest on specific metal nanostructures. The SERS enhancement includes two types: electromagnetic (EM) enhancement[1,2] owing to analytes being adsorbed in vicinity of nanostructures where highly localized electric fields are present and chemical enhancement[3] because of the charge transfer between the analytes and nanostructure. The EM enhancement is currently considered as the dominant process[4].

Illuminated by the light of resonance wavelength, metal nanostructures exhibit strong electromagnetic field enhancements owing to localized surface plasmon resonances and coupled plasmon resonances. Therefore, various SERS substrates have been developed recently. Colloidal suspensions of metal nanoparticles of various shapes and sizes and have been reported[5,6]. They are attractive because of their preparation simplicity, but they have poor reproducibility and environmental stability. Tian group have reported nanoshell and their high sensitivity[7]. Zhang group have proposed pyramidal PMMA structure hybridized with graphene oxide assivated AgNPs that can provide reproducible SERS signals[8]. Nanostructured surfaces with well-controlled dimensions and sharp edges have been reported, such as ultra-sensitive graphene-plasmonic hybrid platform[9], nanopyramids with MoS_2@AgNPs[10] and others[11-13].

Despite the steady progress achieved over the last two decades, there remains strong demand for SERS-active substrates providing a large density of continuous hot-spot sites that possess strong Raman enhancements with high reproducibility and stability. The noble metal triangular-wedge structure has been used as optical waveguide in optic integrated circuit for a long time[14] because of its tighter spatial confinement and higher local field intensity. Even so, the application of the triangular-wedge structure used as SERS substrate hasn't proposed. Many researchers have demonstrated that the electromagnetic field enhancement effect is sensitive to the properties of the noble metal[15] and the wavelength of incident light[16]. In this paper, wedge-enhanced Raman spectroscopy (WERS) substrate is firstly proposed and investigated. The electric field enhancement effect and the effective mode field radius with varying the height of wedge, the vertex angle of wedge, the curvature radius of vertex and the excitation wavelength are analyzed. Compared with the SERS enhancement factor (*EF*) of 5 orders of magnitude on silver gratings that is inspired the local electric field from the top of the substrate[17], that of our Au WERS substrate which is inspired from the side based on guided wave structure can reach up to 10 orders of magnitude. The optimized parameters are obtained and the highest SERS *EF* of Au WERS substrate is 3.171×10^{10}. Moreover, in order to run multiple tests simultaneously on our proposed WERS substrate, the condition for practical application of this substrate is discussed. It reveals that the contact angle φ_c must be in the range of 0°—90° to ensure the detection of liquid sample. With high reproducibility and stability and strong sensitivity, WERS, as a novel Raman enhanced

* This work has been supported by the National Natural Science Foundation of China (No.61905100), and the Fundamental Research Funds for the Central Universities (No.lzujbky-2020-65).

** E-mail: maan@lzu.edu.cn

substrate, will be of great value in biological therapy, chemical detection and biological imaging.

To understand the EM behavior and to approximate the SERS enhancement magnitude of the WERS substrate, the calculation is carried out by the commercial software, which is based on FEM. All plasmonic metals are modeled using the Lorentz-Drude dispersion model[18]. The boundary condition is the scattering boundary condition.

Fig.1(a) illustrates the geometrical structure and parameters that may significantly affect the performance of the WERS substrate. The WERS substrate is composed of three layers: a top layer of Au triangular-wedges, a metal film interlayer and a dielectric layer at the bottom. The structure is taken to be periodic in the X direction. As shown in Fig.1(a), the height of wedge, the vertex angle of wedge and the curvature radius of vertex are denoted as h, θ, r, respectively. Here, the vertex angle of wedge is rounded to avoid field singularities and make the practical fabrication easy for gold[19]. The three most important geometrical parameters that are analyzed in this paper are the vertex of the wedge (θ), the height of wedge (h) and the curvature radius of vertex (r). Higher SERS enhancement factor can be obtained if we optimize these three geometrical parameters. Moreover, the excitation wavelength (λ) is another important parameter which can be tuned for the WERS substrate with the optimal geometric parameters. Fig.1(b) shows the calculated electric field profile of the WERS substrate. The SERS enhancement factor can be inferred from the electric field profile because the enhancement factor are proportional to the biquadrate of the enhancement of the electric field[20]. As shown in Fig.1(b), the electric field is highly focused at the top of Au triangular-wedge. The high electric field is continuously valid along the Z direction, forming uniform and line-shaped hot spots.

In the following parameters analysis, we choose the electric field intensity enhancement effect ($\log E_{loc}$) and the effective mode field radius (R) as two most important physical parameters for optimizing geometrical structures of triangular-wedges. The electric field intensity enhancement effect $\log E_{loc}$ is defined as the logarithm of the electric field intensity at the top of wedge where is the region of strong electromagnetic fields. The effective mode field radius (R) is defined as the distance between the strongest electric field intensity at the top of wedge and the 1/e times of that. Moreover, the radius of curvature is taken as 0.1 nm in order to not only avoid field singularities but also eliminate the influence of the arc process to the vertex angle and height of wedge. More importantly, it is impossible to realize a perfect vertex angle of triangular-wedge in practical fabrication.

Fig.2(a) shows the E-field enhancement characteristics of WERS versus the vertex angle of wedge, θ, which varies from 40° to 90° with fixed aspects h=667 nm, λ=633 nm. It is observed that the electric field enhancement factor $\log E_{loc}$ decreases significantly as the vertex angle of wedge θ increases. Whereas, the effective mode field radius increases with the increase of the vertex angle of wedge. As seen from Fig.2(b), the electric field enhancement factor $\log E_{loc}$ increases observably as the height of wedge increases.

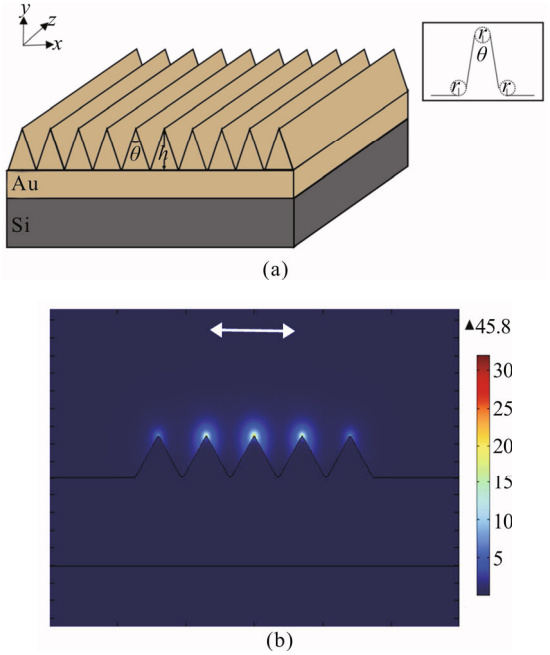

Fig.1 (a) The geometrical structure and (b) the calculated electric field profile of WERS substrate, where the polarization direction of the incident linearly polarized light is denoted by white double-headed arrow

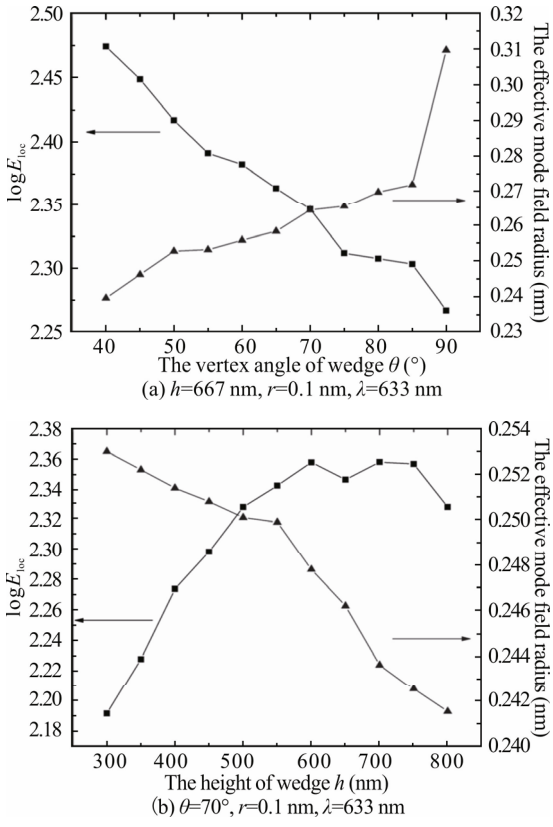

Fig.2 The *E*-field enhancement characteristics of WERS versus (a) vertex angle and (b) height of wedge

Conversely, the effective mode field radius R decreases with the increase of the height of wedge. It can be seen from Fig.3(a) that the electric field enhancement factor $\log E_{loc}$ decreases and the effective mode field radius increases as the arc radius of vertex increases. These above data indicate that while the geometric parameters fixed h=500 nm, θ=70° and the radius of curvature is taken to be ~8 nm, Au wedge can provide the stronger EM enhancement effect and the larger effective mode field radius upon the excitation wavelength λ=633 nm. Here, a 3D simulation was carried out to approximately estimate the excitation wavelength of our proposed Au WERS substrate. As shown in Fig.3(b), it is the electric field intensity enhancement factor $\log E_{loc}/E_0$ and the effective mode field radius R versus the excitation wavelength with fixed h=500 nm, θ=70°, r=8 nm. It is shown that $\log E_{loc}/E_0$ decreases and R increases as the excitation wavelength increases. The results have shown that the intersection of the two curves is 633.37 nm. Therefore, the 633 nm laser is preferred for WERS substrate with fixed h=500 nm, θ=70°, r=8 nm.

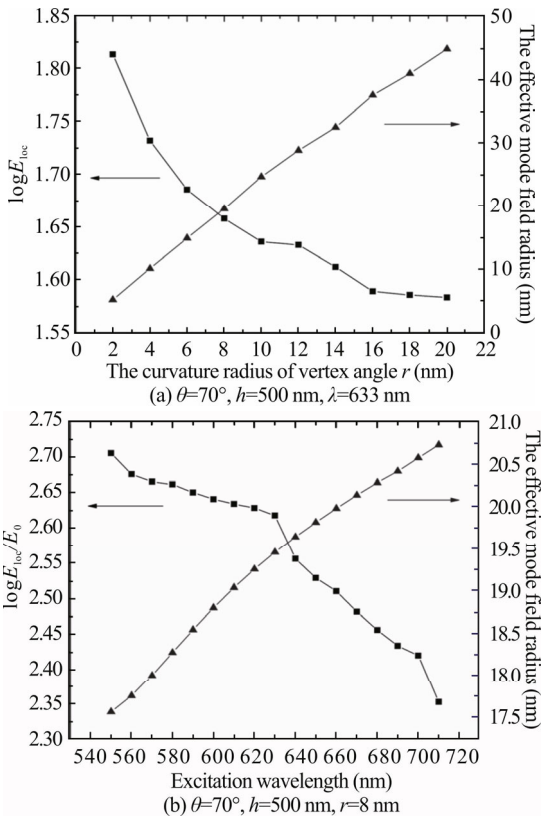

Fig.3 The *E*-field enhancement characteristics of WERS versus (a) curvature radius of wedge and (b) excitation wavelength

To further understand the behavior of the E-field around the top of triangular-wedge, which has a finite radius of curvature, a triangular-wedge structure with varying tip radii is investigated. As shown in Fig.4, a 0.1 nm-radius tip was modeled for comparison with the analytical model, an 8 nm-radius tip was modeled to represent our designed conditions, and a 30 nm-radius tip was modeled for comparison with a blunt tip.

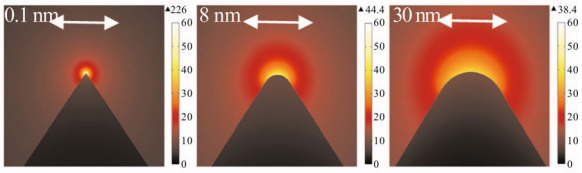

Fig.4 The simulated *E*-field profile of wedge with different curvature radius, where the polarization direction of the incident linearly polarized light is denoted by white double-headed arrow

Moreover, in order to more precisely compare the SERS enhancement factor, we calculate the enhancement factor (EF) of the proposed Au WERS substrate. According to the SERS theory[21], the SERS intensity is proportional to ~$(|E_{loc}|/|E_0|)^4$, so the EF is defined as

$$EF=(|E_{loc}|/|E_0|)^4, \quad (1)$$

where $|E_{loc}|/|E_0|$ is the enhancement of electric field in the hotspots, i.e., the top of triangular-wedge, E_{loc} is the localized field amplitude, E_0 is the incident electric field. The highest SERS EF of the Au WERS substrate can reach up to 3.171×10^{10}. The average SERS EF in the range of effective mode radius range is calculated to be 1.824×10^{10}, which is higher than that of nanostructure proposed by former researchers[16]. Although the enhancement area of our Au WERS substrate is limited, the enhancement effect is extremely high compared with other SERS active platform when the tested samples are located at the proper region. Overall, all these studies indicate that by carefully designing the geometry parameters of Au wedges as well as the excitation wavelength, we can obtain an optimal set of theoretical geometry parameters to detect interested biomolecules under extremely low concentration conditions.

In order to make the most efficient use of this WERS structure, the droplets of the detected sample should attach to the top of wedges rather than in grooves, which means liquid should be wetted on the solid surface[22].

In Fig.5, the contact angle φ_c is a physical parameter of wetting degree. The surface tension between the object, the air and the metal can be used for confirming whether the liquid could wet the solid or not. The surface tensions of solid-gas, solid-liquid, and liquid-gas are defined as γ_{sg}, γ_{sl} and γ_{lg} respectively[23]. The horizontal forces are imbalance, if

$$\gamma_{sg}=\gamma_{sl}+\gamma_{lg}\cos\varphi_c. \quad (2)$$

Eq.(2) is transformed to

$$\cos\varphi_c=(\gamma_{sg}-\gamma_{sl})/\gamma_{lg}. \quad (3)$$

If the surface work of adhesion of the liquid to the solid is

$$w_{ad}=\gamma_{sg}+\gamma_{lg}-\gamma_{sl}. \quad (4)$$

Eq.(4) is converted to

$$\cos\varphi_c = w_{ad}/\gamma_{lg} - 1. \quad (5)$$

When $1<w_{ad}/\gamma_{lg}<2$ ($0°<\varphi_c<90°$) , the liquid is wetting on the surface; when $0<w_{ad}/\gamma_{lg}<1$ ($90°<\varphi_c<180°$), the liquid will not wet the surface. Therefore, $0°<\varphi_c<90°$ should be selected to ensure the droplets deposition.

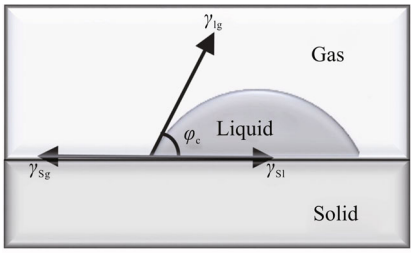

Fig.5 Schematic illustration of the contact angle

In conclusion, a novel Au WERS structure is firstly proposed in this paper. By investigating the electric field enhancement effect and the effective mode field radius with the change of geometry parameters of Au WERS, the optimized parameters are obtained: the vertex angle of wedge is 70°, the height of wedge is 500 nm, the curvature radius of vertex is 8nm and the appropriate excitation wavelength is 633 nm. Under these conditions, the highest EM enhancement factor can reach up to 3.171×10^{10}. The average SERS *EF* in the range of effective mode radius range is 1.824×10^{10}. In addition, the condition for practical application of WERS substrate with large-area arrayed sensing regions is discussed in order to run multiple tests simultaneously. The contact angle φ_c must be in the range of 0°—90° to ensure the detection of liquid sample. The corresponding results reveal that the proposed Au WERS substrate offer a new and practical way to accelerate the development of SERS substrate and will be widely applied in optics, biology, chemistry and other fields.

References

[1] Kneipp J., Kneipp H. and Kneipp K., Chemical Society Reviews **37**, 1052 (2008).

[2] Doering W. E. and Nie S. M., J. Phys. Chem. B **106**, 311 (2002).

[3] Yap F. L., Thoniyot P., Krishnan S. and Krishnamoorthy S., ACS Nano. **6**, 2056 (2012).

[4] Moskovits M., Journal of Raman Spectroscopy **36**, 485 (2005).

[5] Sprague-Klein E. A., McAnally M. O., Zhdanov D. V., Zrimsek A. B., Apkarian V. A., Seideman T., Schatz G. C. and Van Duyne R. P., Journal of the American Chemical Society **139**, 15212 (2017).

[6] Zhan P., Dutta P. K., Wang P., Song G., Dai M., Zhao S. X., Wang Z. G., Yin P., Zhang W., Ding B. and Ke Y., ACS Nano **11**, 1172 (2017).

[7] He Y. H., He R., You E. M., Radjenovic P. M., Sun S. G., Tian Z.Q., Li J. F. and Wang Z. H., Physical Review Letters **125**, 047401 (2020).

[8] Zhao X. F., Yu J., Zhang C., Chen C. S., Xu S. C., Li C. H., Li Z., Zhang S. Z., Liu A. H. and Man B. Y., Applied Surface Science **455**, 1171 (2018).

[9] Wang P., Liang O., Zhang W., Schroeder T. and Xie Y.H., Advanced Materials **25**, 4918 (2013).

[10] Jiang S. Z., Guo J., Zhang C., Li C. H., Wang M. H., Li Z., Gao S. S., Chen P. X., Si H. P. and Xu S. C., RSC Advances **7**, 5764 (2017).

[11] Phan-Quang G. C., Han X., Koh C. S. L., Sim H. Y. F., Lay C. L., Leong S. X., Lee Y. H., Pazos-Perez N., Alvarez-Puebla R. A. and Ling X. Y., Accounts of Chemical Research **52**, 1844 (2019).

[12] Lay C. L., Koh C. S. L., Wang J., Lee Y. H., Jiang R., Yang Y., Yang Z., Phang I. Y. and Ling X. Y., Nanoscale **10**, 575 (2018).

[13] He X., Wang S., Liu Y. and Wang X., Sci. China Chem. **62**, 1064 (2019).

[14] Moreno E., Rodrigo S. G., Bozhevolnyi S. I., Martín-Moreno L. and García-Vidal F. J., Physical Review Letters **100**, 023901 (2008).

[15] Li J. F., Anema J. R., Wandlowski T. and Tian Z. Q., Chemical Society Reviews **44**, 8399 (2015).

[16] Wang Z., Cai K. S., Lu Y., Wu H. N., Li Y. E. and Zhou Q. G., Nanotechnology Reviews **8**, 24 (2019).

[17] Kalachyova Y., Mares D., Lyutakov O., Kostejn M., Lapcak L. and Švorčík V., The Journal of Physical Chemistry C **119**, 9506 (2015).

[18] Trivedi R., Sharma Y. and Dhawan A., Optics Express **23**, 26064 (2015).

[19] Ma A. N., Li Y. E. and Zhang X. P., Plasmonics **8**, 769 (2013).

[20] Stiles P. L., Dieringer J. A., Shah N. C. and Van Duyne R. P., Annual Review of Analytical Chemistry **1**, 601 (2008).

[21] Kneipp K., Wang Y., Kneipp H., Perelman L. T., Itzkan I., Dasari R. and Feld M. S., Physical Review Letters **78**, 1667 (1997).

[22] Hu A. J., Lv B. Z., Wang X. S. and Zhou L., Modern Physics Letters B **30**, 16500781 (2016).

[23] Makkonen L., Journal of Physics: Condensed Matter **28**, 135001 (2016).